VARIATIONS OF THE COASTLINE IN A MEDIUM PERIOD (1985-2017) OF A TROPICAL ISLAND: THE CASE OF SOURE (MARAJÓ - PARÁ/BRAZIL)

Rafael Alexandre Alves Menezes
Diandra Karina Martins Guimarães
Maamar El-robrini

ABSTRACT
The margins of Marajó Island, influenced by large estuaries (Amazonas and Pará rivers), are conditioned to constant geomorphological changes. This article shows the multitemporal dynamics of the coastline (CL 1985-2017 - 32 years) and the quantification of the accretion and erosion areas in the Northern Margin (Sector I), Cabo Maguarí (Sector II) and Eastern Margin (Sector III) of the Soure municipality. The methodology included the acquisition of medium resolution satellite images LANDSAT 5 TM (bands 5, 4 and 3 - 1985) and LANDSAT 8 OLI (bands 6, 5 and 4 - 2017), orthorectified and georeferenced, with spatial resolution of 30m. They were processed using the ArcToolbox tool. The visual interpretation of the images and the vectorization of the CL were done in ArcMap, using the ArcGis 10.6 software. The overlapping of the vectors of the years 1985 and 2017 allowed the CL calculation of areas and rates. The results show the predominance of the accretion of the CL, with a total of 25,382,783.18 m² ± 575.28 m² (4.72 m/year^{-1}) and average linear advancement of 151.10 m. However, the erosion had an area of 6,696,780.64 m² ± 575.28 m² (3.03 m/year^{-1}), with an average linear retreat of 97 m. The erosion and/or accretion processes recorded in the CL of Marajó Island are due to the dynamics in this region (Sectors I, II and III), influenced by the effects of the hydrodynamics of the South Channel of the Amazon River and the Pará River Estuaries.

K**eywords:** Marajó Island; Geoprocessing; Accretion; Erosion.

VARIACIONES DEL COSTERO EN UN PERIODO MEDIANO (1985-2017) DE UNA ISLA TROPICAL: EL CASO DE SOURE (MARAJÓ - PARÁ/BRASIL)

RESUMÉN: Los márgenes de la isla de Marajó, influenciados por grandes estuarios (ríos Amazonas y Pará), están condicionados a constantes cambios geomorfológicos. Este artículo muestra la dinámica multitemporal del litoral (CL 1985-2017 - 32 años) y la cuantificación de las áreas de acreción y erosión en la Margen Norte (Sector I), Cabo Maguarí (Sector II) y Margen Oriental (Sector III) de el municipio de Soure. La metodología incluyó la adquisición de imágenes satelitales de media resolución LANDSAT 5 TM (bandas 5, 4 y 3 - 1985) y LANDSAT 8 OLI (bandas 6, 5 y 4 - 2017), ortorrectificadas y georeferenciadas, con resolución espacial de 30m. Fueron procesados utilizando la herramienta ArcToolbox. La interpretación visual de las imágenes y la vectorización del CL se realizaron en ArcMap, utilizando el software ArcGis 10.6. La superposición de los vectores de los años 1985 y 2017 permitió el cálculo de áreas y tarifas de CL. Los resultados muestran el predominio de la acreción de la CL, con un total de 25.382.783,18 m² ± 575,28 m² (4,72 m/año-1) y un avance lineal promedio de 151,10 m. Sin embargo, la erosión tuvo una superficie de 6.696.780,64 m² ± 575,28 m² (3,03 m/año-1), con un retroceso lineal promedio de 97 m. Los procesos de erosión y/o acreción registrados en el CL de la Isla de Marajó se deben a la dinámica en esta región (Sectores I, II y III), influenciada por los efectos de la hidrodinámica del Canal Sur del Río Amazonas y del Río Pará. Estuarios.

Palabras-Clave: Isla de Marajó; Geoprocesamiento; Acreción; Erosión

INTRODUCTION

A Coastal Zone (CZ) corresponds to the geographical space of interaction between the air, sea, and land, including its renewable or non-renewable resources, encompassing a maritime and a

terrestrial zone (BARAL et al. 2018). The first refers to the space that extends for 12 nautical miles (territorial sea), measured from the baseline (low-tide line). The second is the space defined by the boundaries of municipalities influenced by urbanization, port activity, tourism, and industrial activities (El Robrini et al. 2018a).

The coastline (CL) is used as a geomorphological indicator of coastal dynamics due to its variable position in both time and space (DING et al. 2019, JANA et al. 2014, MAHAPATRA et al. 2014b). Its movement inland reflects retreat or erosion (BARAL et al. 2018). Conversely, its movement offshore or towards the bay represents advance or accretion (DA SILVA et al. 2016a). These changes occur over a medium period, primarily characterized through the analysis of data available in orbital sensor databases (FRANÇA et al., 2007). The main factors influencing the CZ include rainfall, winds, waves, tidal currents, sediment transport and deposition, leading to constant modifications of the CL (AHMED et al. 2021, KANNAN et al. 2014, WANG et al. 2014).

Remote sensing through CL detection technologies is frequently employed to provide information about the CZ morphology. The mosaic of satellite images and CL vectorization emerge as a means to identify variations occurring in the CZ (LUIJENDIJK et al. 2018, MAHAPATRA et al. 2014a, MENTASCHI et al. 2018, MUSKANANFOLA et al. 2020, ORLANDO et al. 2019).

The dynamics of the CL condition slopes that need to be identified and studied from different temporal perspectives, encompassing short, medium, and long-term temporal spatialization (BARAL et al. 2018, BHEEROO et al. 2016, CHENTHAMIL SELVAN et al. 2016, TRAN THI et al. 2014). For this purpose, the acquisition of satellite images and the utilization of Geographic Information System (GIS) environments provide a way to understand the dynamics of the CL over time. This involves data that can be found in numerous databases, making it possible to analyze a large portion of space with satisfactory precision for the analytical component, consequently reducing residual errors, resembling on-site approaches (AL-HATRUSHI 2013, ALESHEIKH et al. 2007, ESMAIL et al. 2019, SANTOS et al. 2021).

Furthermore, the study of coastal geomorphology has enhanced the current scenario, a fact linked to the use of GIS (KALIRAJ et al. 2015, LI et al. 2015; MCFADDEN et al. 2007) and the utilization of a range of satellite images available from the United States Geological Survey (USGS)(FRANÇA er al., 2013; MAHAPATRA et al. 2014a, SANTOS 2017; SOUZA FILHO 2013). The multi-temporal variability of erosion or accretion rates of the CL can be quantified using geospatial techniques. The analysis of these data is employed to understand the dynamics of the CZ, quantifying the rates of variables over

time/space (DE LIMA et al. 2021, ESMAIL et al. 2019, HIMMELSTOSS et al. 2018; MISHRA et al. 2022, MUSKANANFOLA et al. 2020, NASSAR et al. 2019, QUADRADO et al. 2021, STANCHEV et al. 2018).

There are few studies addressing the CL dynamics in the Amazon region, particularly in the Pará state (BAÍA et al. 2021, RANIERI & EL-ROBRINI 2015). This article is part of the plan of the Marine and Coastal Studies Group (GEMC/UFPA), which has been studying the dynamism of the CL of the Amazon since the 90s, and which has already been introduced as new technologies.

Digital Shoreline Analysis System (DSAS), which consists of a complement to the ArcGis software, with the purpose of statistically analyzing the behavior of the CL of a given location, over a certain period. This makes it possible to develop diagnoses. Interest in the factors of CL dynamics (erosion/accretion) allows decision makers to have access to scientific information about coastal kinematics in the study area, where there are few studies on this subject. This dynamic is based on the hypothesis that erosion results from natural processes. Therefore, CL adaptation and preservation planning must rely on knowledge of this dynamic in a context of climate change. This scientific contribution aims to better understand this dynamic for better decision-making by managers of coastal municipalities. Due to the climate change and the vulnerability of ZCs (cities, riverside communities), it is now necessary to develop such monitoring studies, which are useful for decision-making by public authorities.

Two major estuaries, those of the Amazon and Pará rivers, influence the CZ, of the largest fluvio-marine island on the planet (Marajó Island). It undergoes constant morphological changes, imparting a dynamic to the coast based on its geographical position. The study area is located in the eastern part of Marajó Island (PARÁ 2020), influenced by the Pará River Estuary, with physical processes at micro and mesoscales generated by forcings from different sources (astronomical tides and river discharge) (PRESTES et al., 2017, 2020). This stretch comprises the mangrove belt, known as the Amazon Macrotidal Mangrove Coast (AMMC), along 650 km of the CL, extending from Marajó Bay (PA) to Tubarão Point (MA) (SOUZA FILHO 2013).

Thus, comprehending the multi-temporal behavior of the CL contributes to integrated coastal management (PESSOA et al. 2019). However, assessing the evolutionary scenarios of the CZ becomes challenging, as they are subjected to hydrodynamic forcings (waves, tides, sea level oscillation), neotectonics, climate (winds, rains), and human activities (civil and private constructions, deforestation) (AHMED et al. 2021, ATAOL et al. 2019, BOYE et al. 2018, MISHRA et al. 2022; SANTOS

et al. 2021), conditioning geographical space with difficult-to-measure specificities.

This article aims to analyze the multitemporal (1985 to 2017) CL in the western part of the mouth of the Pará River estuary and in the southern channel of the Amazon River.

MATERIALS AND METHODS

Study Area

The research area (136 km along the NE coast of Marajó Island) is located in the Soure CZ, between the Tartarugas channel (Chaves - 0°14'0.67"S/48°55'4.18" W), and the Paracauari River (Salvaterra - 0°44'23.95"S/48°31'14.23"W) (Figure 1). Access can be made by river from the port of Belém to Porto do Camará, covering a distance of 67 km in 2 hours, or by air from Belém Airport to Marajó Island, with a journey in 20 min. Access to the north coast of Marajó Island is possible by air to Macapá, taking 50 min, and/or by river to Chaves, taking 4 hours.

Figure 1. Location of the research area in(Marajó Island). Source: IBGE (2021), USGS (2022), authors (2024).

Characterization of the Study Area

Coastal morphology

The Soure CZ is subdivided into muddy plains (mangroves, cheniers), sandy plain (dunes, barrier-beach ridges, ebb tidal deltas)(EL ROBRINI et al. 2018a). The low-height dunes are distributed on the North and East coasts, located between the beaches and muddy plains, with a preferential

orientation of NNW-SSE and N-S on the East coast (FRANÇA et al., 2007). Barrier-beach ridges consist of linear sandy ridges that extend from the dune belt to the mid-tide line of spring tide. They border the muddy plains and represent a continuous belt of 8.07 km in length on the North edge and 9.47 km at Cabo Maguari. At the mouths of the main tidal channels, ebb tidal deltas occur, formed by a coalescence of sandy (fine to veryfine sands) bars, exposed during low tide, and incised by shallow tidal channels (EL ROBRINI et al. 2018a).

Climatic and Hydrodynamic Data

The research area is characterized by a tropical climate of type Af, with a dry season (June-November) (ALVARES et al. 2014) and a wet season (December-May), presenting a megathermic regime (June). The annual temperatures varies between 18 °C (minimum) and 33 °C (maximum), with an average of 27 °C, and higher values during the dry season (INMET 2024). The average annual rainfall is 2,500 mm. The relative humidity is high throughout the year, ranging between 86 % and 96 % (INMET 2024). In general, the winds average between 6.2 m s^{-1} and 7 m s^{-1} (INMET 2024). However, the winds in this region are the trade winds, coming from the NE, with variations to N and E. The ITCZ undergoes seasonal displacement and reaches the region during the rainy season, with constant and moderate NE trade winds, occasionally gusting up to 9 m s^{-1} (INMET 2024).

The tides have a mesotidal regime, with a height of up to 3.65 m during spring tide (rainy period, January) and 0.5 m during neap tide (April). While the North CL of Marajó Island is under the influence of the hydrodynamics of the South Channel of the Amazon River, with tidal currents of 2 m s^{-1} (GEYER et al. 1991), the East CL is influenced by tidal currents in the Pará estuary river, with velocity of 1.2 m s^{-1} (high tide) and 1.4 m s^{-1} (ebb tide)(ROSÁRIO et al. 2016).

Methodological Procedures

The methodological flow of this research is outlined in Figure 2. The process of selectingthe projection system used involves the consideration of quantifying the data to be generated and using cartographic bases in reference systems with UTM (Universal Transverse Mercator) projections.

Thus, the chosen projection system uses the meter (m) as the unit of measurement to calculate distances and project the position of a component, providing quantitative data specific to the area in question. Furthermore, the vector overlay used was processed in ArcGIS 10.8 software (accessed in the Geographic Information Laboratory-LAIG/UFPA), based on the use of UTM coordinate systems for interpolation in the GIS environment and quantification of the data generated after processing. This is crucial because if it were in another type of projection, it would not be possible to generate the final data, as it would result in processing errors.

Due to the spatial dimension of the area (~120 km), the study area is subdivided into 3 (three) sectors: I) Southern channel of the Amazon River, II) Cabo Maguari, and III) Pará River Estuary.

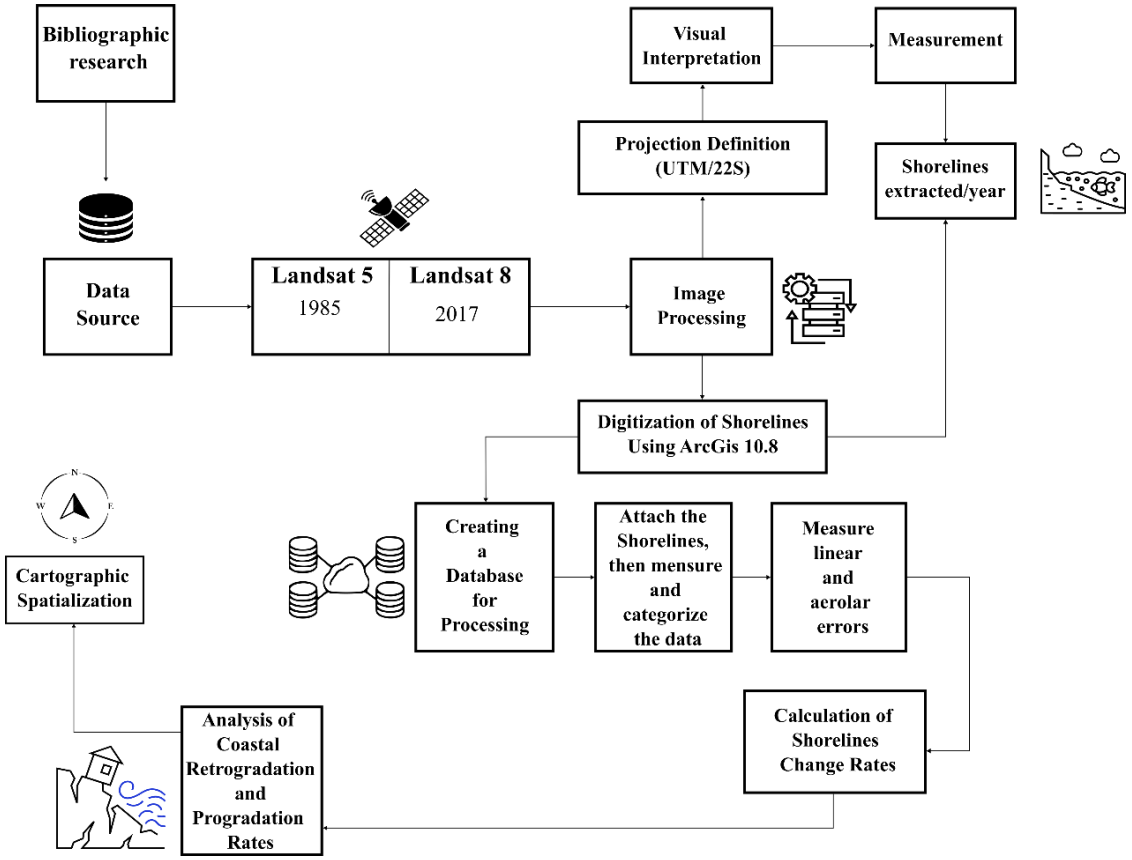

Figure 2. Methodological Flow, authors (2024).

Bibliographic Research

Comparative analyses with similar areas in the Amazon Coastal Zone show trends in accretion and erosion. França et al. (2007), in a study covering the period from 1986 to 2001 (15 years) on the eastern margin of Marajó Island, indicated relatively high values in this sector: accretion, with 148m (16 m/year^{-1}), and erosion, with 192 m (21 m/year^{-1}). It is noteworthy that in this article, the investigated period (1985-2017) is twice as long (32 years) as that considered by França et al. (2003, 2007). The areas in accretion were assessed at 4,602,088.69 m² ± 575.28 m²,and erosion at 2,466,665.80 m² ± 575.28 m², compared to 168,120 m² and 727,804 m².

Thus, Conti and Rodrigues (2011), in a study covering the period from 1973 to 2011 (38 years), show accretion on the western part of Guarás Island (Curuçá), with a 1,300 m advance on Romana Beach, and a tendency for erosion in the central part of the island, with a slow accretion in the eastern part. At Ponta do Picanço (Bragança), Souza Filho and Paradella (2001) calculated the same accretion (1,250 m) as in Curuçá (Conti and Rodrigues, 2011). Furthermore, Ranieri and El-Robrini (2015) concluded that there is a trend of accretion (average rate of 18.24 m/ year^{-1}) and erosion (average rate is 1.62 m/year^{-1}) on the Salinópolis coast, in the period from 1988 to 2013 (25 years). The areas in erosion occur at the boundaries of Corvina-Maçarico and Farol-Atalaia beaches, being more exposed to waves.

On Mosqueiro Island, Guimarães (2019) identified areas in erosion (active cliffs and abrasion platforms), covering 110,879 m² ± 559 m² (3.35 m² year^{-1}), along the Paraíso and Caruara CL. Additionally, there was accretion along the Maraú CL, with a total of 63,971 m² ± 559 m² (1.93 m²/year^{-1}), with restinga occurrence, over the last 33 years (1984-2017).

In a study on the same island (1984 and 2017), Silva (2019) also identified an area with greater erosion covering 13.500 m² ± 559 m² along the Grande CL, while the eroded area on the Bispo CL amounted to only 900 m² ± 559 m². The accretion areas occurred only on the Grande CL, with a total of 5.700 m² ± 559 m². Diniz (2019), in an investigation along the Funda and Saudade beaches (Cotijuba Island, 1984 to 2016/32 years), observed the predominance of erosion (45,357.33 m² ± 707.4m² - 1.71 m/year^{-1}), along the Saudade CL. However, the accretion reaching 8,585 m² ± 707.4 m² (1.09 m/year^{-1}) along the Funda CL. However, at Saudade beach (Rodrigues and Ramos 2013) in the period from 1984 to 2012 (28 years^{-1}), they indicated an accretion of 100 m, with a rate of 3.71 m/year^{-1}, three times higher than the rate calculated for the Funda beach (Diniz 2019). Furthermore, erosion was 3.8 m (1.3571 m/year^{-1}) southwest of the island, the same rate calculated by Diniz (2019). Batista

et al. (2009) reported erosion of 1.37 km²/year^{-1} at Cabo Cassiporé, with a linear average of 27.5 m, and an accretion of 55.85 km² (24.6 m/year^{-1}) at Cabo Orange, during the 1980 - 2003 period (23 years). Recently, El-Robrini et al. (2018b) identified in the Maranhense Gulf; east and west coast of Maranhão, accretion of 79 %, 60 % and 42.9 %, erosion of 6.6 %, 2.8 % and 22.9 %, stability of 79.7 %, 60 %, and 42.9 %, respectively.

Table 1. Accretion and erosion processes in various sectors of the Amazon Coastal Zone: Guarás Island (Curuçá), Eastern margin of Marajó Island, Salinópolis coast, Mosqueiro Island, Cotijuba Island, Cabos Cassiporé and Orange (Amapá), and Maranhão Coast. I: Island, C: Cabos, G: Gulf; Acre. = Accretion, Eros. = Erosion. ALMCL: Average Linear Advance of the CL; TAP: Total Average in accretion; T: Rate; RLMCL: Average Linear retreat of the CL; TÁR: Total Average in erosion, authors (2024).

			Accretion			Erosion		
Authors	**Areas**	**Period**	**ALMCL** (m)	**TAA** (m^2)	**T (m year $^{-1}$)**	**RLMCL (m)**	**TAE (m^2)**	**T (m year^{-1})**
Conti and Rodrigues (2011)	Guarás I. (Curuçá)	1973-2011	1.300	***	***	***	***	***
França et al. (2007)	East Bank of Marajó.	1986-2001	148	168.120	16	192	727.804	21
Ranieri and El-Robrini (2015)	Corvina, Maçarico, Farol-Atalaia (Salinópolis)	1988-2013	***	***	18,24	***	***	1,62
Guimarães(2019)	Paraíso, Caruara e Maraú - Mosqueiro I	1984-2017	62,13	63.971 ± 559	1,93	59,82	110.879 ± 559	3,35
Silva (2019)	Grande, Bispo - Mosqueiro I.	1984-2017	***	5.700 ± de 559	***	***	13.500 ±559 900 ± 559	***
Diniz (2019)	Funda e Saudade - Cotijuba I.	1984-2016	***	8.585 ± 707,4	1,09	***	45.357,33	1,71

							± 707,4	
Batista etal. (2009)	Orange C., Cassiporé C. – Amapá	1980-2003	***	Mangrove 55,85 km²	24,6	27,5	Mangrove 1,37 km²/ano	***
El-Robriniet al. (2018b)	G. Maranhense - Maranhão	2018	79%, 60% e 42,9%		6,6%, 2,8% e 22,9%		79,7%, 60% e 42,9%.	

Satellite Image Acquisition and Spectral Band Composition

In this context, two images were acquired from the LANDSAT 5 TM satellite (09/10/1985) and the LANDSAT 8 OLI (04/12/2017), with spatial resolution of 30 m and 15 m, respectively, after fusion with the panchromatic band (band 8). These images were obtained free of charge through the United States Geological Survey (USGS) website, accessed in February 2017 (Table 2).They are orthorectified and georeferenced, allowing for immediate advancement in the creation of RGB (Red, Green, Blue) compositions of the respective images.

In this regard, ArcMap 10.1 software was used, followed by the ArcToolbox tool, following the path: Data Management Tools > Raster > Data Processing > Composite Bands. Subsequently, the spectral band images were inserted using the path: Input Rasters > Insert bands. In the Landsat 5 image, bands 5, 4, and 3 were used, corresponding to mid-infrared, near infrared, and visible red, respectively. In the Landsat 8 image, bands 6, 5, and 4 were used, corresponding to red, near-infrared, and SWIR1, respectively. After that, band 8 (panchromatic) was inserted into the last image.

To enhance the spectral components of vegetation (Green), a single band was generated for the 1985 and 2017 images by overlaying the previously listed bands. This way, a spectral band highlighting vegetation pigmentation was obtained, from which the vectorization of the CL (shapefile) from the raster (TIFF) will be generated.

Interpretation and Vectorization on Satellite Images

The visual interpretation of the images and the vectorization of the CL were carried out in the ArcMap program of the ArcGIS 10.6 software. The CL was considered as the limit or the contact line between the mangrove and the sandy beach ridges along the Northeastern margin of Marajó Island.

All boundary lines were easily identified in the Landsat images used.

After direct vectorization on the images, the vectors from the years 1985 and 2017 were overlaid. Subsequently, it was possible to generate cartographic and quantitative data: creation of maps, linear measurements, calculation of areas, and rates. The comparison between vectors and quantitative data revealed the temporal mobility of the CL position, the distribution of sectors in erosion, accretion, and the magnitude of erosion and sedimentation over the last 32 years.

Landsat images from 1985 and 2017 were selected, with the lowest possible presence of cloud cover, 18% and 16% respectively, for the analysis of CL changes in Soure (Marajó Island). This choice was justified by the strategic location of Soure, located in the Intertropical Convergence Zone (ZCIT), where monitoring changes in land use and cover is important due to high climatic and environmental dynamics. The minimal presence of clouds in the selected scenes maximizes the clarity and precision of the observations, essential for the detailed assessment of the geomorphological transformations that have occurred on this mangrove coast over the past decade. To ensure the reliability of the data and the accuracy of the results, a cumulative geometricerror was defined between the images used. Considering the georeferencing error of each image, extracted from the metadata and relating it by a rule of three to the pixel value, the cumulative geometric error was obtained as 19.177 m for linear measurements and an error of 575.28 m² for areal measurements (Table 2).

Table 2. Characteristics of Landsat 5 TM (1985) and Landsat 8 OLI (2017) images (path orbit, spatial resolution, bands, pixel error, linear geometric error, areal geometric error), authors (2024).

Images	OrbitPoint	Date	Hour	Spatial Resolution (m)	Bands	PixelError	Linear Geometric Error	Areal Geometric Error
LANDSAT TM 1985	224060	09/10/1985	12:57:54	30	5,4,3	0,326	9,781 m	293,4 m²
LANDSAT OLI 2017	224060	04/12/2017	13:29:01	15	6,5,4,8	0,313	9,396 m	281,8 m²
Cumulative Geometric Error							19,177 m	575,2 m²

RESULTS

Coastline Variation between 1985 and 2017

Through the overlay of vectors (Figure 3), it was possible to perform quantification, revealing the

direction of coastal dynamics (accretion or erosion) during the 1985 to 2017 period (Figure 4). The results indicate the predominance of CL accretion, 25,382,783.18 m² ± 575.28 m² total area (rate of 4.72 m/year^{-1}). The average linear advance of the CL was 151.10 m. while the eroded area reached 6,696,780.64 m² ± 575.28 m² (rate of 3.03 m/year^{-1}). The average linear retreat of the CL was 97 m. The largest accretion areas are located in the northern and northeastern part of Soure, while the largest erosion areas are in the northern and southeastern part of the municipality.

For easier analysis and due to the various dynamic characteristics (erosion, accretion, and stability), the research area was subdivided into three sectors: a) Sector I (northern margin of Soure under the influence of the hydrodynamics of the South channel of the Amazon River); b) Sector II (margin at the confluence of the South channel of the Amazon River and Pará River estuaries – Cabo Maguari); and c) Sector III (eastern margin of Soure under the influence of the Pará River estuary).

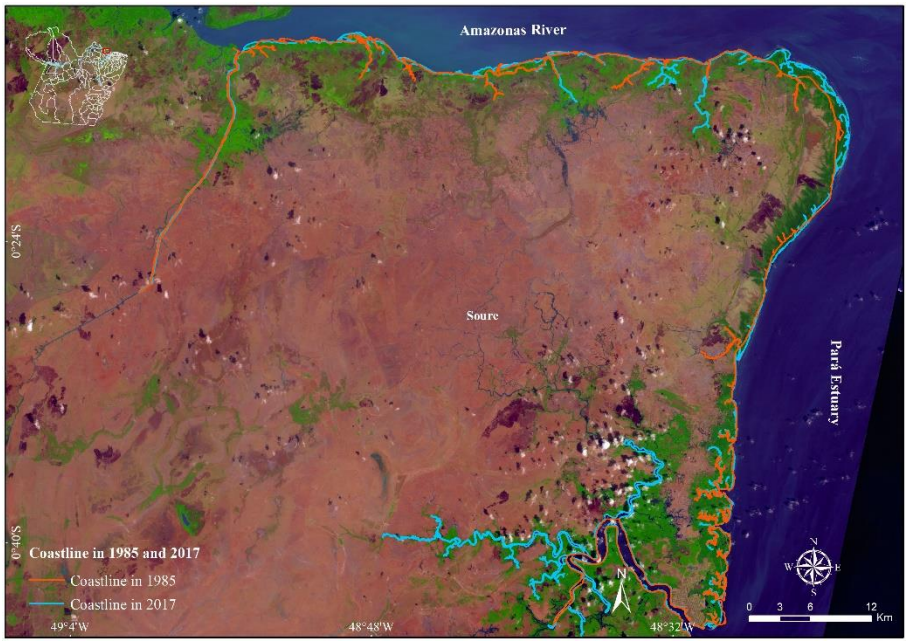

Figure 3. Map showing the overlap of the CL´s from 1985 (red) and 2017 (blue), indicating accretion and erosion areas on the North and East margins of Marajó Island, authors (2024).

Figure 4. Accretion and erosion areas in Sector I (northern margin of Soure) - 1985-2017 period, authors (2024).

Sector I - Northern margin of Soure under the influence of the Southchannel of the Amazon River estuary

The sector I correspond to the northern margin of Soure, stretching 52.1 km from the Turtle Channel to Cabo Maguari, where occur accretion and erosion areas (Figures 5, 6, and 11; Table 3).

Figure 5. Variation in the position of the CL in Sector I (northern margin of the Soure) - 1985 – 2017 period, authors (2024).

Figure 6. Accretion and erosion areas in Sector I (northern margin of Soure) - 1985 – 2017 period, authors (2024).

In this sector, the accretion and erosion areas are almost equivalent, with a slight predominance of accretion, with 4,853,896.10 m² ± 575.28 m² (19 % of the total areas in accretion) of the municipality, with rates of 151,684, 25 m²/year and average linear advance of 4.14 m/year-1. The accreting areas occur in the western part of this sector. However, the areas undergoing erosion are concentrated in the eastern part, with a total of 4,228,224.71 m² ± 575.28 m², and a rate of

132,132.02 m²/year^{-1}. The areas represent 63 % of total erosion. The average linear retreat of the CL was 94.52 m with a rate of 2.95 m/year^{-1}.

Sector II - Margin of the confluence of the South channel of the Amazon River and Pará River Estuaries - Cabo Maguari

The sector II has a length of 19.6 km and is located at the confluence of the South channel of the Amazon River with the mouth of the Pará River estuaries. This sector is predominantly in accretion (Figures 7, 8, and 11; Table 3).

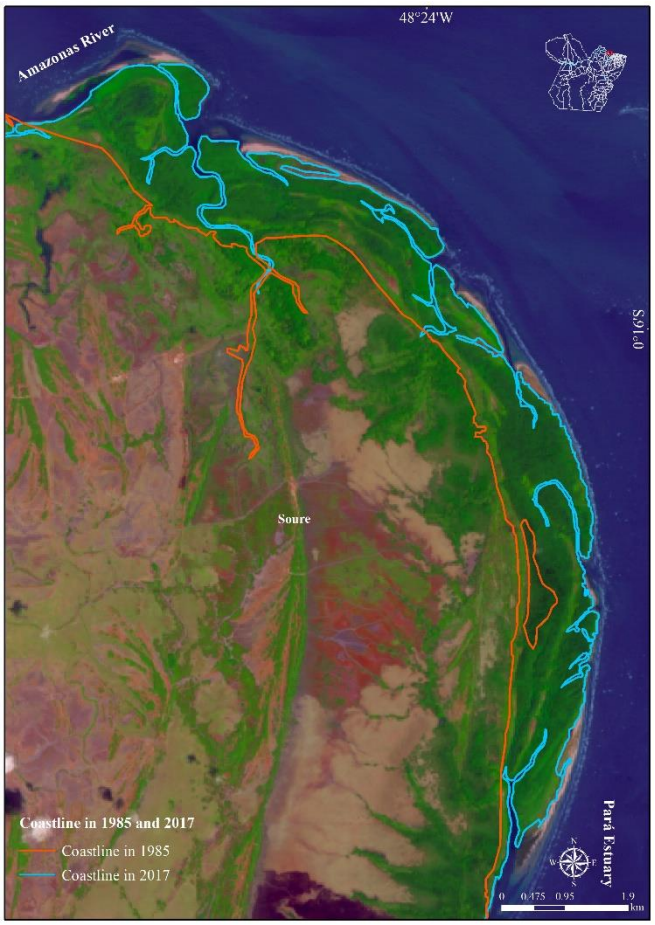

Figure 7. Variation of the CL between 1985 and 2017 in Sector II (confluence of the Amazon River with the Pará River estuaries), in the 1895-2017 period, authors (2024).

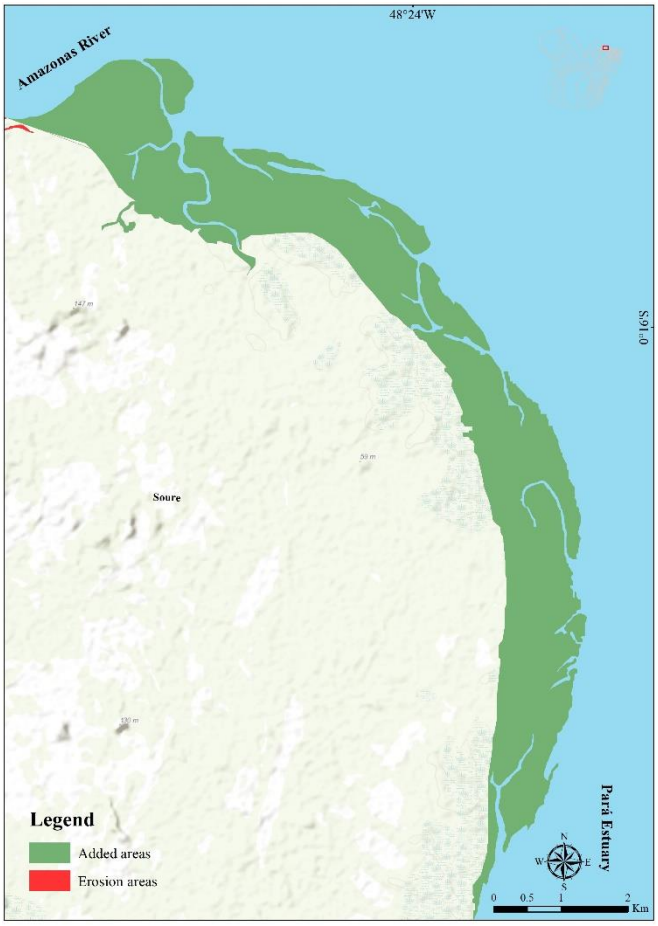

Figure 8. Accretion and erosion areas in Sector II (confluence of the Amazon River and Pará River estuaries) - 1985 – 2017 period, authors (2024).

In this sector, there was accretion of 15,968,622.22 m² ± 575.28 m² with a rate of 499,019.44 $m^2/year^{-1}$. The average linear advance of the CL reached 412.67 m with a rate of 12.90 $m/year^{-1}$. The accretion areas represent 63 % of the total for the municipality.

Sector III – Eastern margin of Soure, under the influence of the Pará River Estuary

The sector III is located on the eastern margin of Soure, between Cabo Maguari and the mouth of the Paracauari tidal channel. It is 50 km long, where there are alternating accretion and erosion areas (Figures 9, 10 and 11; Table 3). The best-known beaches in this northern sector include Turé, Cajuúna, Céu, Pesqueiro, Goiabal, Araruna and Garrote, while to the south is the Soure city.

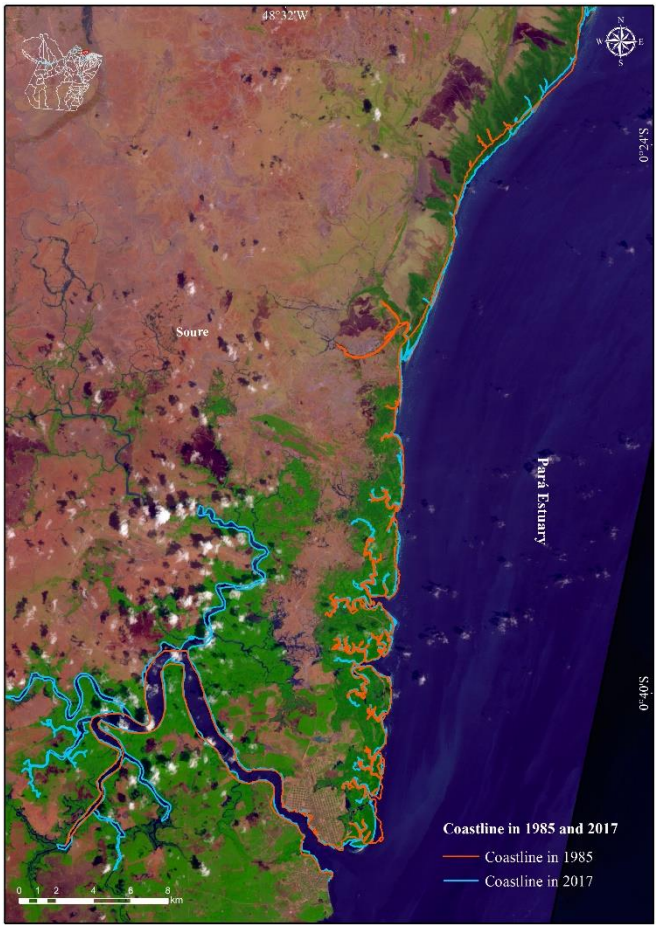

Figure 9. Variation of the CL in Sector III (Eastern margin of Soure), in the 1895-2017 period, authors (2024).

Figure 10. Accretion and erosion areas in Sector III (Eastern margin of Soure) 1985 - 2017 period, authors (2024).

The accreting areas with a total of 4,602,088.69 m² ± 575.28 m², occur mainly in the Northeast and represent 18 % of the accretion area, with a rate of 143,815.27 $m^2/year^{-1}$. The eroded areas, measuring 2,466,665.80 m² ± 575.28 m², occur mainly between the mouths of the Turé and Paracauari tidal channels. These represent 37 % of the total areas under erosion in the municipality, at a rate of 77,083.31 $m^2/year^{-1}$.

The results indicate that, on a medium-term time scale (1985-2017), there was a predominance of LC advancement, leading to the development of accreting areas. Notably, Sector II had the largest accretion area, comprising 63 % of the total area. Sectors I and III represent 19 % and 18 % of the accreting areas, respectively.

Table 3. Quantitative results of CL variation in the municipality of Soure - 1985-2017 period, authors (2024).

	Accretion	Erosion

	Linear Mean Advance of the CL	Total Accretion Area	Mean Linear Retreat of the CL	Total Erosion Area
Sector I	131,41 m	4.853.896,10 m² ± 575,28 m²	94,52 m	4.228.224,71 m² ± 575,28 m²
	4,14 m/year^{-1}	151.684,25 m²/year^{-1}	2,95 m/ year^{-1}	132.132,02 m²/year^{-1}
Sector II	412,67 m	15.968.622,22 m² ± 575,28 m²	-	-
	12,90 m/year^{-1}	499.019,44 m²/year^{-1}	-	-
Sector III	92,40 m	4.602.088,69 m² ± 575,28 m²	98,92 m	2.466.665,80 m² ± 575,28 m²
	2,89 m/year^{-1}	143.815,27 m²/year^{-1}	3,09 m/year^{-1}	77.083,31 m²/year^{-1}
Total	151,10 m	25.382.783,18 m² ± 575,28 m²	97,00 m	6.696.780,64 m² ± 575,28 m²
	4,72 m/year^{-1}	793.211 m²/year^{-1}	3,03 m/year^{-1}	209.274 m²/year^{-1}

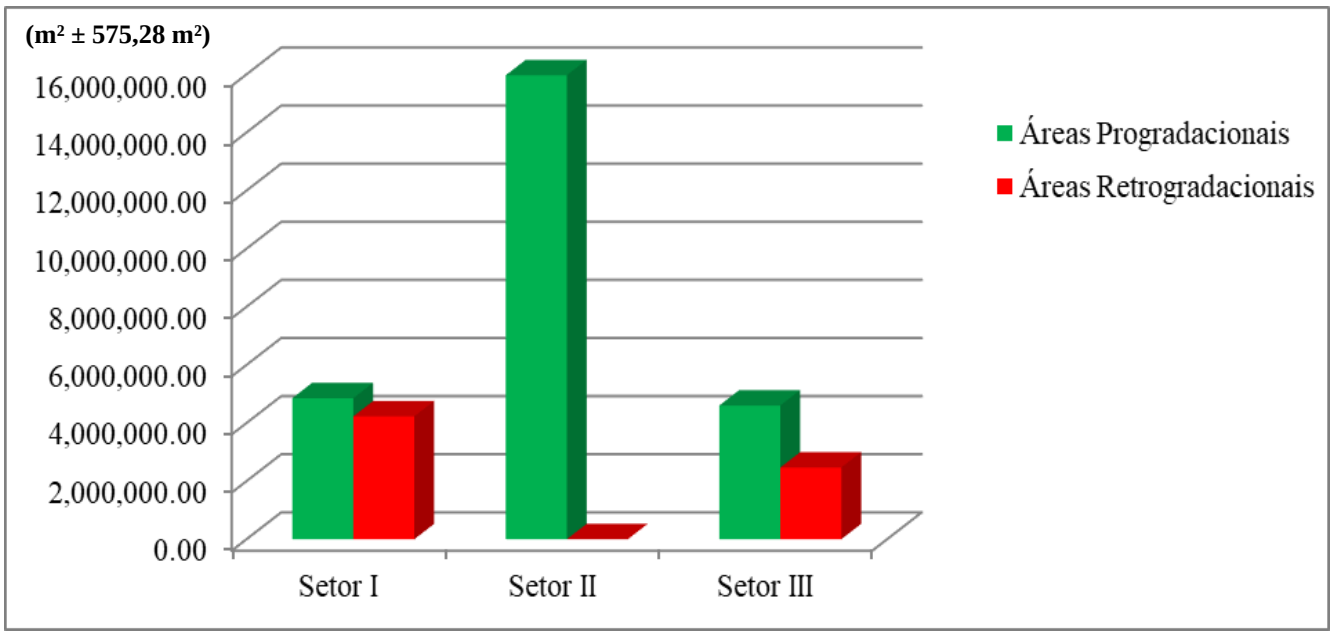

Figure 11. Comparison chart between total accretion and erosion areas in Soure, authors (2024).

In summary, the results indicate that the Accretional process is dominant over the Erosional one. There area quantitative evidence that sector II is being fed by sediments eroded in sectors I and III, resulting in high accretion and expansion of the coastline towards the sea. These data are of utmost importance to understand coastal dynamic processes and for integrated coastal planning purposes.

DISCUSSION

Hydrodynamic conditions directly interfere with the sediment transport process, which is related. Several investigations have revealed that the CL presents a characteristic average shape, called the theoretical equilibrium profile. This equilibrium profile is defined as the "average statistical profile that maintains its shape regardless of small fluctuations, including seasonal ones". The evolution of the equilibrium profile increases exponentially with 12.90 m/year^{-1} from the CL according to the equation h(x) = Axm = 0.67 (DEAN 1977).

In Sector I, the area under erosion is larger than the area under accretion and the sediment balance is negative, with 625,671.39 m² ± 575.28 m² (Table 3). This stretch represents the right bank of the South Channel of the Amazon River Estuary, where 40 % of water and solid discharges flow, featuring high hydrodynamics, resulting in erosion of the CL.

In Sector II, the sediment balance is 100 % positive, as it was exclusively accretionary, with 15,968,622.22 m² ± 575.28 m². Coalescence of sandy bars occurs, with sediments brought by tidal currents from the South Channel of the Amazon River Estuary, the Pará River Estuary and the adjacent continental shelf during high tides.

At the confluence of the South Channel of the Amazon River Estuary with the mouth of the Pará River Estuary, a zone of sediment accumulation originates, influencing the development of a sandy and muddy cape (Cabo Maguari), growing towards the Atlantic Ocean. This results in a large volume of sediment, forming sandy ridges and expanding the mangrove. According to Allison et al. (2000), mangroves directly contribute to the accretion process by providing an additional mechanism for retaining and fixing sediments, acting as "traps" for sediments and serving as protection against waves.

In Sector III, the balance is positive, with 2,135,453.64 m² ± 575.28 m² (Table 3). Tidal currents tend to influence the transport of sediments to this part, in the Pará River Estuary, close to Cabo Maguari. Although the North and East margins of Marajó Island are influenced by different hydrodynamic conditions of the Amazon River (Sector I) and the Pará River Estuaries (Sector III), the areas under erosion had almost the same linear retreat, respectively 94.52 m (2.95 m/year^{-1}) and

98.92 m (3.09 m/year^{-1} over a period of 34 years). However, the accretion areas were much larger in Sector I, with a linear advance of 131 m (4.14 m/year^{-1}) compared to Sector III, with 92.40 m (2.89 m/year^{-1}). Meanwhile, Sector II suffered accretion, with the largest linear advance of 412.67 m (12.90 m/year^{-1}).

In general, the west coast shows a tendency to erosion due to the erosive effects in the South Channel of the Amazon River Estuary, where strong tidal currents due to macro tides (maximum 4.2 m during spring tide, with a variation of 0.5- 1.2 m at neap tide) (ROSÁRIO et al. 2016). The Pará River Estuary presents an intense fluvial contribution combined with the co-oscillation of astronomical tides, resulting in a differentiated hydrodynamic pattern and a complex mixing process.

The sediments on this margin consist mainly of medium to fine sand (CORRÊA 2006). Another factor to consider is that this CL is more exposed to winds that penetrate the South Channel at speeds of 2 m/s and 7 m/s (INMET 2024), contributing to greater erosion.

FINAL CONSIDERATIONS

The methodology employed, based on semi-automatic methods extracted from the spatial analysis of orbital images acquired by remote sensors (Landsat), and using vector overlay, allowed significant progress from a scientific perspective for the Amazon region and with global importance. Throughout the paper, geoprocessing tools and techniques are utilized, which can be replicated in other CZ and contribute to technical, theoretical, andmethodological support for management policy makers.

The challenges of implementing this set of techniques are numerous. However, the acquisition of a more precise temporal and spatial dataset with less cloud presence stands out, whichbecomes almost unfeasible due to the study area being in the ITCZ. An alternative to overcome this perspective could be the use of active sensors (synthetic aperture radar) and/or photogrammetry from unmanned aerial vehicles (UAVs), integrating them with the available data enabled in this study and in others from the perspective of this manuscript.

The CL is very dynamic and its position changes in space on temporal scales (millennial, secular, decadal, seasonal) and can be influenced by several processes, which may be natural, due to coastal dynamics (sea level oscillation, sediment balance, events extremes, water/solid discharge), and/or anthropogenic (dredging, construction, hydroelectric power, damming of rivers).

Depending on the action of these processes, the CL can migrate offshore (accretion), retreat towards the island (erosion), or remain stable. In the case of the Marajó island, erosion does not

imply the destruction of the sandy beaches, what is observed is that the beach has been retreating into the island.

With the results, it was possible to identify that each area of the sector is marked by a different dynamic according to its exposure to coastal factors. Thus, the achieved results arerelevant, as public administrator´s considering that the sectors on the eastern margin of Soure do not exhibit the same dynamics throughout their extension can use the analysis.

Despite significant progress in this work, more in-depth analyses of the processes controlling the retreat and accretion of the CL in this geographic space are still needed. Given that the information obtained in this study summarizes only a few parameters (statistical rates and mobility of the CL) of the dynamics, it is suitable for case studies (in loco). Particularly, seeking a greater acquisition of recent oceanographic and geological data, as well as a set of orbital data, as this region is still subject to few integrated studies in relation to these areas of scientific knowledge,to evaluate possible predictions of evolutionary scenarios of the CL.

Finally, the analysis conducted on this region, integrated with the processes that act on the CL of Marajó Island, is just a fragment for understanding a more complex dynamic. However, it can contribute as a subsidy for future prospecting on the coastal dynamics of other regions, adding informational mechanisms that serve as a model for predicting environmental changes, over a large temporal and spatial scale, using remote sensing and geoprocessing techniques.

ACKNOWLEDGMENTS

This study was financed in part by the Coordination for the Improvement of Higher Education Personnel – Brazil (CAPES) – Finance Code 001. Dr. Carmena Ferreira de França for her theoretical and methodological contribution.

REFERENCES

AHMED, N.; Howlader, H.; Hoque, M.; Pradhan, B. Coastal erosion vulnerability assessment along the eastern coast of Bangladesh using geospatial techniques. Ocean & Coastal Management, v, 199, p. 105408-0.1016, 2021.

AL-HATRUSHI, S. M. *Monitoring of the shoreline change using remote sensing and GIS: a case study of Al Hawasnah tidal inlet, Al Batinah coast, Sultanate of Oman*. Arabian Journal of Geosciences, v. 6, n. 5, p. 1479–1484, 14 maio 2013.

ALESHEIKH, A. A.; GHORBANALI, A.; NOURI, N. *Coastline change detection using remote sensing*. International Journal of Environmental Science & Technology, v. 4, n. 1, p. 61–66, 1 dez. 2007.

ALLISON, M.A.; LEE, M.T.; OGSTON, A.S.; ALLER, R.C. *Origin of Amazon mud banks along the northeastern coast of South America*. Mar. Geol. 163: 241-256. 2000.

ALVARES, C.A.; STAPE, J.L.; SENTELHAS, P.C.; GONÇALVES, J.L. de M.; SPAROVEK, G. Köppen's. *Climate classification map for Brazil.* Meteorologische Zeitschrift, Vol. 22, n° 6: 711-728.2014.

ATAOL, M.; KALE, M. M.; TEKKANAT, I. S. *Assessment of the changes in shoreline using digital shoreline analysis system: a case study of Kizilirmak Delta in northern Turkey from 1951 to 2017.* Environmental Earth Sciences, v. 78, n. 19, 2019.

BAÍA, L. B.; RANIERI, L. A.; ROSÁRIO, R. P. *Análise multitemporal da variação da linha de costa em praias estuarinas do Nordeste do Pará.* Geociências, v. 40, n. 1, p. 231–244, 2021.

BATISTA, E. da M.; SOUZA FILHO, P.W.M.S.; SILVEIRA, O.M.da. *Avaliação de áreas deposicionais e erosivas em cabos lamosos da zona costeira Amazônica através da análise multitemporal de imagens de sensores remotos*. Rev. Bras. Geof., v. 27, supl. 1: 83-96. 2009.

BERTACCHINI, E. *Map updating and coastline control with very high resolution satellite images: application to Molise and Puglia coasts (Italy)*. Italian Journal of Remote Sensing, p. 103–115, 30 jun. 2010.

BHEEROO, R. A.; *Chandrasekar, N.;Seenipandi, K.; Magesh N.S. Shoreline change rate and erosion risk assessment along the Trou Aux Biches–Mont Choisy beach on the northwest coast of Mauritius using GIS-DSAS technique*. Environmental Earth Sciences, v. 75, n. 5, p. 444, 3 mar. 2016.

BOYE, C. B. et al. *Spatio-temporal analyses of shoreline change in the Western Region of Ghana*. Journal of Coastal Conservation, v. 22, n. 4, p. 769–776, 2018.

Baral, R.; Samal, R.N.; Mishra, S.K. Shoreline Change Analysis at Chilika Lagoon Coast, India Using Digital Shoreline Analysis System July 2018Journal of the Indian Society of Remote Sensing, v. 46(3), p. https: DOI:10.1007/s12524-018-0818-7.

Chenthamil, S.; Kankara, R.S.; Markose, V.J.; Rajan, B.; Prabhu, K. Shoreline change and impacts on coastal protection structures on Puducherry, SE coast of India. Natural Hazards, 83, 293. https://doi.org/10.1007/s11069-016-2332-y.

CONTI, L.A.; RODRIGUES, M. *Variação da Linha de costa na ilha dos Guarás através de análise de série temporal de imagens de satélites.* Revista Brasileira de Geografia Física, n° 5: 922-937. 2011.

CORRÊA, I.C.S. *Aplicação do Diagrama de Pejrup na Interpretação da Sedimentação e da Dinâmica do Estuário da Baía de Marajó*. Pesquisas em Geociências, Porto Alegre, v. 32, n° 2: 109-118. 2006.

DA SILVA, G. V.; Muler, M.; Prado, M.F.V.; Short, A.D.; Klein, A.H.F.; Toldo, E.E., Jr. Shoreline change analysis and insight into the sediment *Shoreline Change Analysis and Insight into the Sediment Transport Path along Santa Catarina Island North Shore, Brazil.* Journal of Coastal Research, v. 320, p. 863–874, jul. 2016b.

De Lima, L.T.; Fernández-Fernández, S.; Espinoza, J.M. De A.; Albuquerque, M. Da G.; Bernardes,

C. End Point Rate Tool for QGIS (EPR4Q): Validation Using DSAS and AMBUR. ISPRS Int. J. Geo-Inf. 2021, 10, 162. https://doi.org/10.3390/ijgi10030162.

Dean, R.G. *Equilibrium Beach Profiles: Characteristics and Applications*. Journal of Coastal Research, Vol. 7, n° 1, p. 53-84, 1991. https://www.jstor.org/stable/4297805.

DHN (Diretoria de Hidrografia e Navegação). *Tábuas de maré*. Disponível em: https://www.marinha.mil.br/chm/tabuas-de-mare. Acesso em: 3 de janeiro de 2023.

Ding, X.S.; Shan, X.J.; Chen, Y.L.; Jin, X.S.; Muhammed, F.R. Dynamics of shoreline and land reclamation from 1985 to 2015 in the Bohai Sea, China. J. Geogr. Sci., 29, 2031–2046. 2019.

DINIZ, L.M. *Dinâmica costeira das orlas Funda e Saudade, Ilha de Cotijuba: análise multitemporal da posição da linha de costa (1984 e 2016) e indicadores atuais.* Trabalho de Conclusão de Curso, Faculdade de Geografia, Universidade Federal do Pará: 92p. 2019.

ESMAIL, M.; MAHMOD, W. E.; FATH, H. *Assessment and prediction of shoreline change using multi-temporal satellite images and statistics: Case study of Damietta coast, Egypt.* Applied Ocean Research, v. 82, p. 274–282, 1 jan. 2019.

EL-ROBRINI, M.; RANIEIRI L. A.; SILVA, P.V.M.; GUERREIRO, J.S.; ALVES, A.M. da S.; OLIVEIRA, R.R.S. da; SILVA, M. do S.F. da.; AMORA, P.B.C.; EL ROBRINI, M. H.S.; FENZL, N. Panorama da erosão costeira no Pará. In: Panorama da erosão costeira no Brasil. Editor emChefe: Muehe, D. ISBN: 978.85.7738.394-8: 65-165. 2018.

EL-ROBRINI, M.; SANTOS, J.H.S. dos; LIMA, L.G.de; SANTOS, A.L.S. dos; Santos, M.C.F.V. dos; SOUZA, U.D.V. *Panorama da Erosão Costeira no Maranhão*. In: Panorama da erosão costeira no Brasil: Editor em Chefe: Muehe, D. ISBN: 978.85.7738.394-8: 19-63. 2018.

FRANÇA, C.F. De; SOUZA FILHO, P.W.M.; EL-ROBRINI, M. *Análise faciológica e estratigráficada planície costeira de Soure (margem leste da ilha de Marajó), no trecho compreendido entre o canal do Cajuúna e o estuário Paracauari*. in Acta Amaz, vol. 37, n °2: 261-268. 2007.

GEYER W.R.; BEARDSLEY, R.C.; CANDELA, J.; CASTRO, B.M.; LEGECKIS, R.V.; LENTZ, S.J.; LIMEBURNER, R.; MIRANDA, L.B.; TROWBRIDGE, J.H. *The Physical Oceanography of the Amazon Outflow*. Oceanography-April: 8-14. 1991.

GUIMARÃES, D.K.M., *Análise de Indicadores de Dinâmica Costeira da Orla do Paraíso, Caruara e Maraú entre 1984 e 2017, Ilha de Mosqueiro, Belém.* Trabalho de Conclusão de Curso. Faculdade de Geografia, Universidade Federal do Pará: 63p. 2019.

Himmelstoss, N.A.; Schuster, S.; Hutzler, F.; Moran, R.; Hawelka, S. *Digital Shoreline Analysis System (versão 5.0); Um ArcGIS © extensão para o cáclulo alteração na linha costeira: lançamento do software U.S.* Disponível em: <https://code.usgs.gov/cch /dsas>. Acesso em: 20 maio. 2020.

INMET, Instituto Nacional de Meteorologia. *Normais climatológicas do Brasil 1961-2020.* Disponível em: http://www.inmet.gov.br/portal/index.php?r=clima/normaisclimatologicas. Acesso em 10 de janeiro de 2024.

JANA, A.; Arkoprovo, B.; Sabyasachi, M.; Bhattacharya, A.K. *Shoreline changes in response to sea level rise along Digha Coast, Eastern India: an analytical approach of remote sensing, GIS and statistical techniques*. Journal of Coastal Conservation, v. 18, n. 3, p. 145–155, 22 jun. 2014. DOI:

10.1007/s11852-013-0297-5.

KALIRAJ, S.; CHANDRASEKAR, N.; MAGESH, N. S. *Evaluation of coastal erosion and accretion*

processes along the southwest coast of Kanyakumari, Tamil Nadu using geospatial techniques. Arabian Journal of Geosciences, v. 8, n. 1, p. 239–253, 10 jan. 2015.

KANNAN, R.; Anand, K. V.; Sundar, V.; Sannasiraj, S. A.; Rangarao, V. *Shoreline changes along the Northern coast of Chennai port, from fieldmeasurements*. ISH Journal of Hydraulic Engineering, v. 20, n. 1, p. 24–31, 2014. DOI: 10.1080/09715010.2013.821789.

Li, X.; Zhou, Y.; Tian, B.; Kuang, R.; Wang, L. GIS-based methodology for erosion risk assessment of the muddy coast in the Yangtze Delta, Ocean & Coastal Management, Vol. 108, 97-108, 2015.

https://doi.org/10.1016/j.ocecoaman.2014.09.028.

LUIJENDIJK, A.; Hagenaars, G.; Ranasinghe, R.; Baart, F.; Donchyts, G.; Aarninkhof. *The State of the World's Beache*s. Scientific Reports, v. 8, n. 1, p. 6641, 27 dez. 2018. DOI: 10.1038/s41598-018-24630-6.

MAHAPATRA, M.; RATHEESH, R.; RAJAWAT, A. S. *Shoreline Change Analysis along the Coastof South Gujarat, India, Using Digital Shoreline Analysis System.* Journal of the Indian Society of Remote Sensing, v. 42, n. 4, p. 869–876, 2014.

MCFADDEN, L.; Nicholls, R.J.; Vafeidis, A.; Tol, R.S.J. *A Methodology for Modeling Coastal Space for Global Assessment*. Journal of Coastal Research, v. 234, p. 911–920, jul. 2007. https://doi.org/10.2112/04-0365.1.

Mentaschi, L.; Vousdoukas, M.I.; Pekel, J.; Voukouvalas E.; Feyen, L. 2018. Global long-term observations of coastal erosion and accretion. Scientific Reports, v. 8, n. 1, p. 12876, 27 dez. 2018.

Mishra, M., Acharyya, T., Chand, P., Santos, C. A. G., Kar, D., Das, P. P., Nascimento, T. V. M. do. Analyzing shoreline dynamicity and the associated socioecological risk along the Southern Odisha Coast of India using remote sensing-based and statistical approaches. Geocarto International, 37(14), 3991–4027, 2022. https://doi.org/10.1080/10106049.2021.1882005.

MUSKANANFOLA, M. R.; SUPRIHARYONO; FEBRIANTO, S. *Spatio-temporal analysis of shoreline change along the coast of Sayung Demak, Indonesia using Digital Shoreline Analysis System*. Regional Studies in Marine Science, v. 34, p. 101060, 2020.

Nassar, K.; Mahmod, W.E.; Fath, H.; Masria, A.; Nadaoka, K.; Negm, A. *Shoreline change detection using DSAS technique: Case of North Sinai coast, Egypt*. Marine Georesources & Geotechnology, v. 37, n. 1, p. 81–95, 2 jan. 2019. https://doi.org/10.1080/1064119X.2018.1448912.

ORLANDO, L.; ORTEGA, L.; DEFEO, O*. Multi-decadal variability in sandy beach area and the role of climate forcing.* Estuarine, Coastal and Shelf Science, v. 218, p. 197–203, 5 mar. 2019.

PARÁ. *L.ei n° 9.064*, de 25 de maio de 2020.

PESSOA, R. M. C.; Manoel, R.; Quintana, J.; Antonio, J.; Rauquírio Marinho, Da C.M.; Pereira, C.C.L. *Federal conservation units in the Brazilian amazon coastal zone: An adequate approach to control recreational activities?* Ocean & Coastal Management, v. 178, p. 104856, ago. 2019.

PRESTES, Y. O.; Silva, A.C.; Rollnic, M.; Rosário, R.P. *The M2 and M4 tides in the Pará River Estuary.* Tropical Oceanography, v. 45, n. 1, p. 26-37, 7 maio 2017. https://doi.org/10.5914/tropocean.v45i1.15198et al.

PRESTES, Y. O.; Borba, T.A. Da C.; Silva, A.C. Da; Rollnic, M. A discharge stationary model for the Pará-Amazon estuarine system, Journal of Hydrology: Regional Studies, Volume 28, p. 100668, 2020.

https://doi.org/10.1016/j.ejrh.2020.100668.

QUADRADO, G. P.; Dillenburg, S.R.; Goulart, E.S.; Barboza, E.G. Historical and geological assessment of shoreline changes at an urbanized embayed sandy system in Garopaba, Southern Brazil. Regional Studies in Marine Science, V. 42, p. 101622, 2021. https://doi.org/10.1016/j.rsma.2021.101622.

RANIERI, L.A.; EL-ROBRINI, M. *Evolução da linha de costa de Salinópolis, Nordeste do Pará, Brasil.* Pesquisas em Geociências, v. 42, n° 3: 207-226. 2015.

RODRIGUES, S.W.P.; RAMOS, E.M.L.S. *Detecção de mudanças do litoral da ilha de Cotejuba.* In: ANAIS DO XVI SIMPÓSIO BRASILEIRO DE SENSORIAMENTO REMOTO, Foz do Iguaçú, 13-18, 2013.

ROSÁRIO, R.P.; BORBA, T.; SANTOS, A.S.; ROLLNIC, M., *Variability of Salinity in Pará RiverEstuary: 2D Analysis with Flexible Mesh Model.* Conference: International Coastal Symposium, Journal of Coastal Research, Volume: SI 75: 128-132. 2016.

SANTOS, C. A. G.; Nascimento, T.V.M. Do; Mishra, M.; Silva, R.M. Da. Analysis of long- and short-term shoreline change dynamics: A study case of João Pessoa city in Brazil. Science of The Total Environment, V. 769, p. 144889, 2021. https://doi.org/10.1016/j.scitotenv.2020.144889.

SOUZA FILHO, P. W. M. E. *Costa de maguezais de macromaré da amazônia: cenários morfológicos, mapeamento e quantificação de áreas usando dados de sensores remotos*. Revista Brasileira de Geofísica, v. 53, n. 9, p. 1689–1699, 2013.

SILVA, R.R.P. A*nálise da Variação da Linha de Costa (1984-2017) e Indicadores da Orla Grande-Bispo.* Trabalho de Conclusão de Curso. Faculdade de Geografia, Universidade Federal do Pará: 63p. 2019.

STANCHEV, H.; Stancheva, M.; Young, R.; Palazov, A. Analysis of shoreline changes and cliff retreat to support Marine Spatial Planning in Shabla Municipality, Northeast Bulgaria. Ocean & Coastal Management, v. 156, p. 127–140, abr. 2018. https://doi.org/10.1016/j.ocecoaman.2017.06.011.

SOUZA FILHO, P.W.M.; PARADELLA, W.R. Synthetic Aperture Radar for Coastal Erosion Mapping, and Land-Use Assessment in the Moist Tropics: Bragança Coastal Plain Case Study. In: Anais X SBSR, Foz do Iguacu, 21-26 abril 2001, INPE, Sessão Técnica Oral - Workshop: 339-347.

USGS (United States Geological Survey). *Landsat Collection 2 level 1.* Disponível em: https://earthexplorer.usgs.gov/ Acesso em: 02 de Janeiro de 2019.

TRAN THI, V.; Xuan, T.T.; Phan Nguyen, H.; Dahdouh-Guebas, F.; Koedam, N. *Application of remote sensing and GIS for detection of long-term mangrove shoreline changes in Mui Ca Mau, Vietnam*. Biogeosciences, 11, 3781–3795, 2014. https://doi.org/10.5194/bg-11-3781-2014.

WANG, Y.; Xiyong, H.; Mingming, J.; Ping, S.; Liangju, Y. *Remote Detection of Shoreline Changes in Eastern Bank of Laizhou Bay, North China*. Journal of the Indian Society of Remote Sensing, v. 42, n. 3, p. 621–631, 12 set. 2014. DOI: 10.1007/s12524-014-0361-0.

SOBRE OS AUTORES / AUTORAS

Rafael Alexandre Alves Menezes. Universidade Federal do Pará. Email: rafa.menezes1996@gmail.com

Diandra Karina Martins Guimarães. Universidade Federal do Pará. https://orcid.org/0000-0002-8894-5783. Email: guimaraesdiandra@gmail.com

Maamar El-robrini. Doutor em Geologia Marinha, Professor do Programa de Pós-Graduação em Oceanografia (PPGOC). Universidade Federal do Pará. https://orcid.org/0000-0001-7850-1217. Email: robrinigmc@gmail.com